Physics Letters A 379 (2015) 3045–3049

Contents lists available at ScienceDirect

Physics Letters A

www.elsevier.com/locate/pla

Robust quantum gates between trapped ions using shaped pulses

Ping Zou, Zhi-Ming Zhang *

Guangdong Provincial Key Laboratory of Nanophotonic Functional Materials and Devices (SIPSE), and
Guangdong Provincial Key Laboratory of Quantum Engineering and Quantum Materials, South China Normal University, Guangzhou 510006, China

ARTICLE INFO

Article history:
Received 1 August 2015
Received in revised form 24 September 2015
Accepted 10 October 2015
Available online 20 October 2015
Communicated by A. Eisfeld

Keywords:
Quantum computation
Quantum gate
Trapped ion
Shaped pulse
State dependent force
High fidelity

ABSTRACT

We improve two existing entangling gate schemes between trapped ion qubits immersed in a large linear crystal. Based on the existing two-qubit gate schemes by applying segmented forces on the individually addressed qubits, we present a systematic method to optimize the shapes of the forces to suppress the dominant source of infidelity. The spin-dependent forces in the scheme can be from periodic photon kicks or from continuous optical pulses. The entangling gates are fast, robust, and have high fidelity. They can be used to implement scalable quantum computation and quantum simulation.

1. Introduction

The trapped ion system is an ideal platform to implement quantum computation and quantum simulation for its long coherence time, high controllability, efficient initialization and measurement [1–3]. The two-qubit entangling gate in trapped ion system is mediated by collective motion modes of the ions [4–11]. For a large numbers of ions within a single crystal there will be many crosstalk motional modes. If we only use a single mode to implement the gate, the gate speed will significantly slow down because of the small frequency splitting of the motional modes. To overcome the problem, schemes in which qubits are simultaneously coupled to multimode of motion by applying qubit state-dependent optical forces are proposed [6–9]. Then the errors from the mode crosstalk are suppressed without slowing down the gates. The scheme in [8,9] has been demonstrated within a chain of five trapped ion with high fidelity entangling gates [11]. In the scheme, qubits are individually addressed by segmented optical pulses in a programmable way. $2N+1$ pulse segments are sufficient to get unit fidelity on any two ions in an N ion chain and less segments may be found by a searching algorithm in computer to get near-unit fidelity with suitable parameters.

A significant source of infidelity in the schemes using multiple modes is the presence of residual qubit-motion entanglement at the end of the gate operation, leading to decoherence and a degradation of the fidelity of entanglement generation. Some schemes are proposed [8–10,12,13] to suppress this kind of error and improve gate fidelity. Using the similarity between the procedure of removing the influence of the motional mode here and that of maintaining the coherence of a quantum system from the influence of the environment, a phase modulated decoupling scheme [12] is proposed. This scheme is closely related to the concatenated dynamical decoupling (CDD) sequence [14,15]. However, the number of pulse segments required grows exponentially with the number of modes, and with increasing order of error suppression. Here, we describe an alternative general strategy to decouple qubits from multiple intermediary motional modes. Our scheme is related to the Uhrig dynamical decoupling (UDD) sequence [16,17]. The number of the pulse segments will only grows linearly with increasing order of error suppression. The gates are achieved by segmented forces on the individually addressed qubits as in [8,9], but instead of the nonlinear search approach, we propose a systematic one to optimize the shapes of the forces to suppress the dominant source of infidelity to arbitrary order. Furthermore, our scheme can be applied to both the ultrafast gate [6,7] and fast gate [9,11].

2. The trapped ion system

The system is a set of N ions confined in a linear trap and subjected to some external spin-dependent forces. Assume that harmonic trapping potentials characterized by the center-of-mass (c.m.) trap frequencies (ω_x, ω_y, ω_z) are approximately equal in the

* Corresponding author.
E-mail addresses: zouping@m.scnu.edu.cn (P. Zou), zmzhang@scnu.edu.cn (Z.-M. Zhang).

http://dx.doi.org/10.1016/j.physleta.2015.10.014
0375-9601/

two transverse directions $\omega_x \approx \omega_y$, and that the ratio $\beta = \omega_{x,y}/\omega_z$ is larger than the critical value $0.73N^{0.86}$ such that the ions form a linear chain along the axial direction z [18]. If the spin-dependent force is applied along the x direction, then the Hamiltonian can be written as

$$H = H_0 + \sum_{n=1}^{N} F_n(t) x_n \sigma_n^z, \tag{1}$$

where $H_0 = \sum_n T_n + \sum_n V_n^T + \sum_{n,l} V_{nl}^C$ accounts for the kinetic energy T_n, trapping potentials V_n^T summarized over all ions, and the Coulomb interaction V_{nl}^C between every pair of ions n and l. x_n is the small displacement of the ion n from its equilibrium position in direction $\hat{x}$ and $F_n(t)$ is the time-dependent external force on ion n. The force also depends on the internal state of the ion. After expanding H_0 around the equilibrium configuration and diagonalization, the Hamiltonian can be rewritten in terms of the normal phonon modes

$$H = \sum_k [\hbar\omega_k (a_k^\dagger a_k + 1/2) - \sum_{n,k} g_{n,k} F_n(t)(a_k^\dagger + a_k)\sigma_n^z]. \tag{2}$$

Here, ω_k is the eigen-frequency of motional mode k in the x direction, $a_k(a_k^\dagger)$ is the corresponding lowing (raising) operator of mode k, $g_{n,k} = \sqrt{\frac{\hbar}{2M\omega_k}} b_{n,k}$, and $b_{n,k}$ is the normal mode transformation matrix for ion n and mode k [2]. The evolution operator of the interaction Hamiltonian is [8]

$$U(\tau) = \exp(\sum_n \phi_n(\tau)\sigma_n^z + i \sum_{l,n} \chi_{l,n}\sigma_l^z \sigma_n^z), \tag{3}$$

here, the first term corresponds to the qubit motion coupling on ion n, where $\phi_n(\tau) = \sum_k [\alpha_{n,k}(\tau) a_k^\dagger - \alpha_{n,k}^*(\tau) a_k]$, and $\alpha_{n,k}(\tau)$ is the amount of the state-dependent displacement of ion n in phase space of the kth motional mode

$$\alpha_{n,k}(\tau) = \frac{i g_{n,k}}{\hbar} \int_0^\tau F_n(t) e^{i\omega_k t} dt. \tag{4}$$

The second term in Eq. (3) is the interaction between qubit l and n, with

$$\chi_{l,n} = \frac{2}{\hbar^2} \sum_k g_{l,k} g_{n,k} \int_0^\tau dt' \int_0^{t'} dt F_l(t) F_n(t') \sin[\omega_k (t - t')]. \tag{5}$$

A non-trivial two-qubit gate $U_{a,b} = \exp[i\pi\sigma_a^z\sigma_b^z/4]$ on two arbitrary ions a and b, which is equivalent to the controlled phase gate by single-qubit rotations, can be accomplished by applying identical spin-dependent forces on only these two ions with $F_a(t) = F_b(t) = F(t)$, if $\chi_{a,b}(T_g) = \pi/4$ and $\alpha_{a,k}(T_g) = 0$ for all the modes k, where T_g is the total gate time. This means that the qubits must be decoupled from all motional modes after the gate operation. The constraints can be satisfied by evenly partitioning the pulse shape $F_l(t) = F_n(t) = F(t)$ into $2N + 1$ segments, reducing the problem to a system of linear equations with guaranteed solution [8,11]. Although fewer pulse segments for high fidelity gate may be found by a search algorithm, much more segments will be needed to implement the gate when N increases. Here, we present a general strategy to find segmented pulse shape to decouple qubits from the motional modes to arbitrary order. In this scheme, for large ion number N the number of the pulse segment is not too large for experimental implementation. Depending on the concrete force producing methods, our scheme can be applied to both the cases of ultrafast gate with speed orders of magnitude faster than the trap period and fast gate with time several or tens of the transverse trap period.

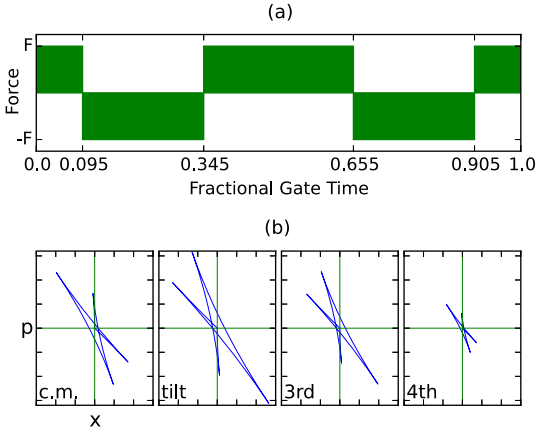

Fig. 1. (Color online.) (a) The segmented pulse pattern, parameterized by the time point at which the force direction is reversed. The force amplitude F is to be determined by the equation $\chi_{a,b} = \pi/4$. (b) Phase space trajectories (arbitrary units but all on same scale) for the pulse pattern in (a) applied to ion pair 1 and 2 in a four ion chain with $\omega_x/2\pi = 4.0$ MHz, $\beta = 10$ and $T_g = 0.01$ μs.

3. Ultrafast gate

We first consider the state-dependent forces produced by coherent photon kicks from fast laser pulses, which can be used to implement two-qubit gate orders of magnitude faster than the trap period [6,7]. A pair of short Raman pulses with the wave vector $\boldsymbol{k}_1$ and $\boldsymbol{k}_2$ applied on ion i and j will give a state-dependent momentum kick $\hbar(\boldsymbol{k}_1 - \boldsymbol{k}_2)\sigma_\alpha^z$ $(\alpha = i, j)$ to the ions for each π rotation of the state $|0\rangle_\alpha$ and $|1\rangle_\alpha$ (this pair of Raman pulses is denoted by their directions $(\boldsymbol{k}_1, \boldsymbol{k}_2)$). If we alternatively apply the Raman pulses in the $(\boldsymbol{k}_1, \boldsymbol{k}_2)$ and $(-\boldsymbol{k}_1, -\boldsymbol{k}_2)$ directions and each pulse sequence is periodic with a repetition frequency $f_r/2$ much larger than the ion trap frequency, then the net effect can be well approximated by a continuous kicking force F with mean magnitude $F = \sqrt{2}\hbar k_c f_r$ along the radial axis $\hat{\boldsymbol{x}}$. Here we assume that $\boldsymbol{k}_1 \perp \boldsymbol{k}_2$, $|\boldsymbol{k}_1| = |\boldsymbol{k}_2| = k_c$, and both wave vectors have a 45° angles to direction $\hat{\boldsymbol{x}}$. To lead to ultra-fast gate design, the implementation of this spin-dependent force beyond the Lamb–Dicke limit, requires a non-trivial frequency comb based technique invented in [22]. We use the transverse phonon (TP) modes to demonstrate the strategy and it also works for the longitudinal phonon (LP) modes. Below $\omega_{c.m.}$ denotes the c.m. eigen-frequency in $\hat{x}$ direction.

In the gate operation, to eliminate or reduce the noise part given by Eq. (4), a sequence of iterated basic cycle is designed in [7]. Here we reformulate the result and provide more pulse sequences which may be a better potential for suppress the residual qubit-motion entanglement. We alternatively apply the kicking force F and the force $-F$ in the reverse direction on the pair of ions as shown in Fig. 1(a). The pulse is divided into $J + 1$ subintervals. The durations of the subinterval are not equal and the instants to change the force direction are $T_g \sin^2(\pi j/(2J + 2))$ with $j \in \{1, 2, \cdots, J\}$. At the end of the gate operation, the residual qubit-motion entanglement $\alpha_{a,k}$ will be order $O((\omega_{c.m.} T_g)^{J+1})$. Then we can calculate the gate fidelity using the definition described in [8,10]

$$F_g = \frac{1}{8}[2 + 2(\Gamma_a + \Gamma_b) + \Gamma_+ + \Gamma_-], \tag{6}$$

where $\Gamma_{a(b)} = \exp[-\sum_k |\alpha_{a(b)}^k(T_g)|^2 \bar{\beta}_k/2]$ and $\Gamma_\pm = \exp[-\sum_k |\alpha_a^k(T_g) \pm \alpha_b^k(T_g)|^2 \bar{\beta}_k/2]$. The parameter $\bar{\beta}_k$ is given by $\bar{\beta}_k = \coth(\hbar\omega_k/2k_B T)$, with k_B denoting the Boltzmann constant. The infidelity of the gate is defined as $F_{in} = 1 - F_g$.

The deriving of the optimal instants is similar to the UDD decoupling pulse sequence. The total time interval of the gate time

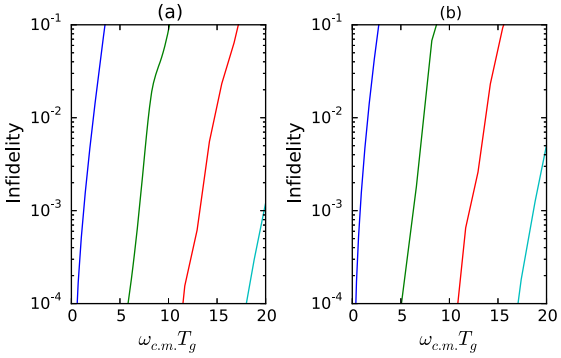

Fig. 2. (Color online.) The infidelity versus time for various numbers of segments with thermal phonon number $\bar{n}_{c.m.} = 0.1$ in (a) and $\bar{n}_{c.m.} = 2$ in (b). The segments number is 4, 8, 12, 16 respectively from left to right. The pulses are applied to ion pair 1 and 2 within a 20 ion chain with $\omega_x/2\pi = 4.0$ MHz and $\beta = 10$.

is split into smaller intervals $0 \to \delta_1 T_g \to \delta_2 T_g \cdots \to \delta_J T_g \to T_g$ with $0 < \delta_1 < \delta_2 < \cdots < \delta_J < 1$. At each time point $\delta_j T_g$ the force change its direction. By summing the integral of each segment the displacement in phase space of Eq. (4) is given by $\alpha_{a,k}(T_g) = -\frac{g_{a,k}F}{\hbar\omega_k} y_J(\omega_k T_g)$, where

$$y_J(z) = 1 + (-1)^{J+1}e^{iz} + 2\sum_{j=1}^{J}(-1)^j e^{iz\delta_j}. \tag{7}$$

The aim is to optimize the J instants $\{\delta_j\}$ such that $y_J(z)$ is as small as possible. One way to do so is to make the first J derivatives of $y_J(z)$ vanish. Notice that $y_J(0)$ is always equal to 0. The mth derivative reads

$$\frac{d^m}{dz^m} y_J(z)|_{z=0} = -i^m[(-1)^{J+1} + 2\sum_{j=1}^{J}(-1)^j \delta_j^m]. \tag{8}$$

Thus we have a set of equations

$$(-1)^{J+1} + 2\sum_{j=1}^{J}(-1)^j \delta_j^m = 0 \tag{9}$$

for $m \in \{1, 2, \cdots, J\}$. The solutions can be easily found analytically as $\delta_j = \sin^2(\pi j/(2J+2))$ [16].

For $J = 2$, it is the basic cycle used in [7], with no more constraint on the gate time T_g. To get higher-order pulse, the basic cycle and π pulse are combined in [7]. Here, we obtain more higher-order pulse sequences. They are the pulses with $J > 2$, and they may be used to simplify the experiment, because they have less segments than the pulse combining the pulse with $J = 2$ and π pulse for the same infidelity order. Furthermore, we can also combine the pulse with $J > 2$ and the π pulse to get more pulse sequences. In Fig. 1(a) we present a five-segment sequence. The amplitude of the force F is to be determined by the constraint $\chi_{a,b}(T_g) = \pi/4$. When the operation is applied on the fist two ions in a four ion chain with $\omega_x/2\pi = 4.0$ MHz, $\beta = 10$ and $T_g = 0.01$ μs, the repetition frequency f_r is about 1.2 GHz. In Fig. 1(b) we present the phase trajectories of the motional modes during the gate operation between the first two ions in a four ion chain. At the end of the operation, all the trajectories are back to their origins, so all the motional modes are simultaneously disentangled from the qubits. Fig. 2 shows that sequence is insensitive to the ions' temperature by comparing the fidelities with different thermal phonon number, and that $\omega_{c.m.}T_g$ can be in a larger range with the gate preserving high fidelity if the segment number increases, which may make the experiments flexible in choosing experiment parameters.

4. Fast gate

Great progress has been made in the past years in controlling the fast laser pulse to induce a series of coherent photon kicks [20–22], However, the more realistic way to implement entangling gates today is to use continuous forces, which have been demonstrated in several experiments [11,19]. In the experiments, a state-dependent optical force at frequency μ can be produced by generating bichromatic beat notes near the upper and lower motional sideband frequencies at $\omega_0 \pm \mu$, where ω_0 is the frequency splitting of the qubit, and the detuning μ is in the neighborhood of the motional mode frequencies. Assuming the modes in x direction within the Lamb–Dicke limits and using the rotating wave approximation, the force $F(t)$ takes the form $F(t) = \hbar\delta k_x \Omega(t)\sin(\mu t)$, where $\Omega(t)$ is the time-dependent Rabi frequency, and δk_x is the wave vector difference along direction x. Note that motion modes in axial z direction need not be confined within the Lamb–Dicke limits [9]. Based on this type of spin-dependent force, the method to obtain the pulse shape for the two-qubit gate $U_{a,b}$ has been discussed in detailed in [8–10]. The Laser pulse is partitioned into uniform segments of constant intensity, then the gate infidelity is minimized by optimizing the intensities. The optimizing procedure is performed by a searching algorithm in computer. Here we propose a systematic procedure. Our method will reduce the number of segments in the situation where many segments are needed using the searching algorithm [8]. If the gate time is faster than the trap period, for example, $(\omega_{c.m.} + \mu)T_g$ is of order 1 or below, we can follow the step from Eq. (7) to Eq. (9) after expanding $\sin(\mu t)$ in $F(t)$ as $(e^{i\mu t} - e^{-i\mu t})/2i$. However for short gate time, the maximum of Rabi frequency $\Omega(t)$, i.e. the optical power need to be sufficient strong. We then modify the above scheme to make the gate be performed with moderate Rabi frequencies which current experimentally technique can reach. In the ultrafast gate scheme, the utilization of the TP modes for gate operation is not necessary, while with our continuous scheme, it is necessary. One major feature of the TP modes is that the eigen-frequencies spectrum is much tighter than that of the LP modes [9]. Because of the small frequency splittings in TP mode, resolving a particular TP mode is difficult for a large ion array. Thus it is necessary to go beyond the sideband addressing (single-mode) limit to achieve a high-speed gate. All the phonon modes are accounted to design high-fidelity gates with fast speed [9,11]. Here we further demand that all the eigen-frequencies of motional modes are sufficiently close. In the experiments, this tight degree of the frequency spectrum can be controlled by the trap frequency ratio β and ω_z. The gap between the highest c.m. mode frequency and the lowest zigzag mode frequency in x direction $\delta\omega_x = \omega_{x,c.m.} - \omega_{x,zz}$ decreases when β increasing or ω_z decreasing as [23]

$$\delta\omega_x = \omega_z\left[\beta - \sqrt{\beta^2 + \frac{1}{2} - \frac{1}{2}u_{z,zz}}\right] \tag{10}$$

where $u_{z,zz} = \left(\frac{\omega_{z,zz}}{\omega_z}\right)^2$ is only dependent on the ion number N, and $\omega_{z,zz}$ is the frequency of the zigzag mode in the axial z direction. We need $\delta\omega_x T_g$ be small, and the details will be described below.

In this modified scheme, we still partition the pulse shape into $J+1$ segments (shown in Fig. 3(a)). But now the pulse segment durations are set to be equal, while the relevant Rabi frequencies unequal. The time points to change Rabi frequency therefore are $\delta_j T_g = jT_g/(J+1)$ $(j \in \{1, 2, \cdots, J\})$. The relevant Rabi frequencies of the segments are denoted by Ω_k $(k = 0, 1, \cdots J)$ respectively. The detuning μ is set to be the middle of the spectrum of the $\hat{x}$ direction, $\mu = (\omega_{c.m.} + \omega_{zz})/2$, and the gate time is constrained to be one of a series of discrete values $m(J+1)\frac{\pi}{\mu}$, where m is an

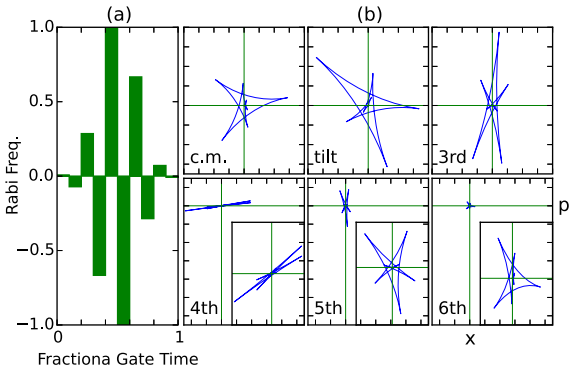

Fig. 3. (Color online.) (a) The segmented pulse pattern, parameterized by the Rabi frequency $\Omega(t)$. In the figure the relative values for different segments are shown, and the absolute amplitude is to be determined by the equation $\chi_{a,b} = \pi/4$. (b) Phase space trajectories (arbitrary units but all on the same scale) for the pulse pattern in (a) applied to ions 1 and 2 within a six ion chain with $\omega_x/2\pi = 3.0$ MHz, $\beta = 25$ and $T_g = 158.88$ μs. The enlarged views of the three in the bottom are also presented.

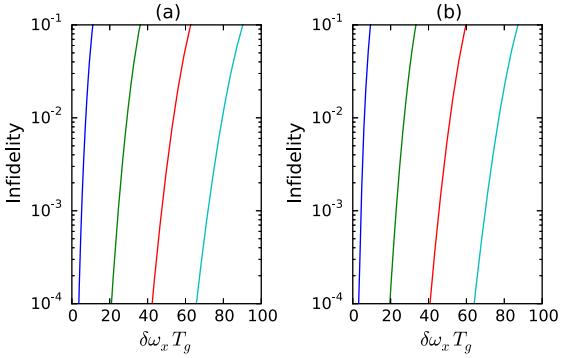

Fig. 4. (Color online.) The infidelity versus $\delta\omega_x T_g$ for various numbers of segments. The infidelity is for the entangling gate between the ion pair 1 and 2 within a 10 ion chain in (a) and within a 20 ion chain in (b) with $\omega_x/2\pi = 3.0$ MHz. The segment number is 5, 10, 15, 20 respectively from left to right. In the calculating, we assume that thermal phonon number $\bar{n}_{c.m.} = 2$. The gate times T_g are all about 100 μs, and the precise values need be determined by the constraint described in text. $\delta\omega_x$ is controlled by β or ω_z.

integer. The above parameters are chosen such that $(\omega_k - \mu)T_g$ is around 0, and $(\omega_k + \mu)T_g$ around $2m\pi(J+1)$. Again $\alpha_{a,k}$ in Eq. (4) can be calculated by summing the integral of each segment

$$\alpha_{a,k}(T_g) = \frac{g_{a,k}}{2i\hbar}\left(\frac{y_J((\omega_k+\mu)T_g)}{\omega_k+\mu} - \frac{y_J((\omega_k-\mu)T_g)}{\omega_k-\mu}\right), \tag{11}$$

where

$$y_J(z) = -\Omega_0 + \sum_{j=1}^{J}(\Omega_{j-1} - \Omega_j)e^{i\delta_j z} + \Omega_J e^{iz}. \tag{12}$$

The aim is to optimize the $J+1$ Rabi frequencies $\{\Omega_j\}$ such that $y_J(z)$ is as small as possible around two points, $z = 0$ and $z = 2m\pi(J+1)$. Notice that $y_J(0) = 0$ and $y_J(2m\pi(J+1)) = 0$ for any sequence $\{\Omega_j\}$. Similarly, one way to do so is to make the first J derivatives of $y_J(z)$ vanish at both $z = 0$ and $z = 2m\pi(J+1)$. Actually both constraints give the same set of J linear equations of Ω_j

$$\sum_{j=1}^{J}(\Omega_{j-1} - \Omega_j)\delta_j^s + \Omega_J = 0, \tag{13}$$

where $s = 1, 2, \cdots, J$. Combining with the requiring $\chi_{a,b} = \pi/4$, all Ω_j can be easily determined. By controlling the experiment apparatus and experiment parameters described above, $\alpha_{a,k}(T_g)$ will be the order $O(|(\omega_k+\mu)T_g - 2m\pi(J+1)|^{J+1}) + O(|(\omega_k-\mu)T_g|^{J+1})$. Fig. 3(a) presents a ten-segment sequence, and Fig. 3(b) shows the phase trajectories of the motional modes during the period when the sequence is applied to the first two ions in a six ion chain, again at the end of the operation, all the motional modes are simultaneously disentangled from the qubits. Fig. 4 depicts the relation between the tight degree of eigen-frequencies $\delta\omega_x$ and the number of segments when the gate preserving high fidelity. If more pulse segments are used, the tight degree of the motional modes can be released. Note that keeping the maximum amplitude of the Rabi frequency fixed, the limit of $\chi_{a,b}(T_g)$ as $\delta\omega_x$ approaches to zero is also zero because of the orthogonality of the matrix $b_{n,k}$, then to implement the gate, higher laser power will be needed. The number of segments should be appropriately determined by the experiment constraints. For an example, a gate infidelity of 7.6×10^{-6} is obtained if a 10 segmented pulse sequence is applied to the ion pairs 1 and 2 in a 20 ion chain with $\beta = 80$, $\omega_x/2\pi = 3$ MHz, $\delta\omega_x/2\pi = 0.0166$ MHz and gate time $T_g = 158.773$ μs. The value of $g_{a,k}$ of the c.m. mode is set as 0.0158, then the maximum amplitude of the Rabi frequency is $\Omega_{max}/2\pi = 1.0414$ MHz. This gate time is less than the experimental gate time 190 μs within a five ion chain in [11]. When the number of trapped ions increase, the number of needed segments increases slowly. For example, pulse with 15 segments is enough for a gate on the first ion pairs in a 50 ion chain, with infidelity 4.0×10^{-4}, gate time $T_g = 76.07$ μs and the maximum amplitude of the Rabi frequency $\Omega_{max}/2\pi = 3.482$ MHz. In a similar way, we can also combine the above pulse shape with the π pulse. For example, in the 20 ion chain, instead of the pulse with $J = 9$ (10 segments), using two pulses with $J = 4$ applied on the pair of ions sequentially with the direction of the second reversed, we can also get low infidelity gate with $F_{in} = 7.5 \times 10^{-5}$, gate time $T_g = 58.495$ μs and $\Omega_{max}/2\pi = 4.025$ MHz. Because of the higher-order approximation, small fluctuations of μ or ω_x will not make sensible change to $\alpha_{a,k}(T_g)$, so the gate will be robust to these fluctuations.

5. Conclusion

We have proposed a systematic and optimal shape modulating method to implement high fidelity two-qubit gate with trapped ions. The scheme can works in both the ultrafast and fast gate time regions. By taking more pulse, the fidelity of the gate increases. When the number of trapped ions increase, the segment number increases slowly. This scheme is much less sensitive to ion heating and thermal motion outside of the Lamb–Dicke limit. The gate is also robust to the fluctuations in the trap frequency ω or detuning μ. We hope our shape modulating pulse sequences are useful for improving the entangling gate fidelity.

Acknowledgements

We thank Ya-Fei Yu for helpful discussions. This work was supported by the Major Research Plan of the NSFC (Grant No. 91121023), the NSFC (Grant Nos. 61378012 and 60978009), the SRFDPHEC (Grant No. 20124407110009), the 973 Project (Grant Nos. 2011CBA00200 and 2013CB921804), and the PCSIRT (Grant No. IRT1243).

References

[1] J.I. Cirac, P. Zoller, Phys. Rev. Lett. 74 (1995) 4091.
[2] D.F.V. James, Appl. Phys. B 66 (1998) 181.
[3] D. Leibfried, R. Blatt, C. Monroe, D. Wineland, Rev. Mod. Phys. 75 (2003) 281.
[4] A. Sørensen, K. Mølmer, Phys. Rev. Lett. 82 (1999) 1971.

[5] G.J. Milburn, S. Schneider, D.F.V. James, Fortschr. Phys. 48 (2000) 801.
[6] J.J. García-Ripoll, P. Zoller, J.I. Cirac, Phys. Rev. Lett. 91 (2003) 157901.
[7] L.-M. Duan, Phys. Rev. Lett. 93 (2004) 100502.
[8] S.-L. Zhu, C. Monroe, L.-M. Duan, Europhys. Lett. 73 (2006) 485.
[9] S.-L. Zhu, C. Monroe, L.-M. Duan, Phys. Rev. Lett. 97 (2006) 050505.
[10] G.-D. Lin, S.-L. Zhu, R. Islam, K. Kim, M.-S. Chang, S. Korenblit, C. Monroe, L.-M. Duan, Europhys. Lett. 86 (2009) 60004.
[11] T. Choi, S. Debnath, T.A. Manning, C. Figgatt, Z.-X. Gong, L.-M. Duan, C. Monroe, Phys. Rev. Lett. 112 (2014) 190502.
[12] T.J. Green, M.J. Biercuk, Phys. Rev. Lett. 114 (2015) 120502.
[13] A.M. Steane, G. Imreh, J.P. Home, D. Leibfried, New J. Phys. 16 (2014) 053049.
[14] K. Khodjasteh, D.A. Lidar, Phys. Rev. Lett. 95 (2005) 180501.
[15] K. Khodjasteh, D.A. Lidar, Phys. Rev. A 75 (2007) 062310.
[16] Götz S. Uhrig, Phys. Rev. Lett. 98 (2007) 100504.
[17] Götz S. Uhrig, New J. Phys. 10 (2008) 083024.
[18] A. Steane, Appl. Phys. B 64 (1997) 623.
[19] K. Kim, M.-S. Chang, R. Islam, S. Korenblit, L.-M. Duan, C. Monroe, Phys. Rev. Lett. 103 (2009) 120502.
[20] W.C. Campbell, J. Mizrahi, Q. Quraishi, C. Senko, D. Hayes, D. Hucul, D.N. Matsukevich, P. Maunz, C. Monroe, Phys. Rev. Lett. 105 (2010) 090502.
[21] D. Hayes, D.N. Matsukevich, P. Maunz, D. Hucul, Q. Quraishi, S. Olmschenk, W. Campbell, J. Mizrahi, C. Senko, C. Monroe, Phys. Rev. Lett. 104 (2010) 140501.
[22] J. Mizrahi, C. Senko, B. Neyenhuis, K.G. Johnson, W.C. Campbell, C.W.S. Conover, C. Monroe, Phys. Rev. Lett. 110 (2013) 203001.
[23] D.G. Enzer, et al., Phys. Rev. Lett. 85 (2000) 2466.